Dynamics of a Vapor Bubble in Film Boiling and the Superheat Effect

FELLA CHOUARFA[1], ABIDA BAHLOUL[2], M.E.HOCINE BENHAMZA[1], SAMIRA BOUFAS[1]
[1]Laboratory of Industrial Analysis and Materials Engineering,
University May 8, 1945 Guelma,
P.O. Box 401 Guelma, 24000,
ALGERIA

[2]Laboratory of Computational Chemistry and Nanostructures,
University May 8, 1945 Guelma,
P.O. Box 401 Guelma, 24000,
ALGERIA

Abstract: - This study aims at developing an improved numerical simulation of the film boiling regime phenomenon to understand and visualize the growth of vapor bubble at a heated surface during low and high superheats. The simulation of the bubble dynamics including the bubble growth, departure, coalescence, rising, and frequency of detachment under different wall superheats is numerically investigated. The continuity, momentum, and energy equations are solved for the two immiscible fluids phases using the finite volume method. The phase change model and the results exhibited a good agreement with the theoretical models. The obtained results show that the velocity of bubble growth and its frequency of emission promotes heat exchange. It is found that the shape of a bubble has been influenced by the wall superheat. It is also found that the high superheat generates a large amount of steam in which the steam bubble takes the shape of a fungus. So, a clear correlation exists between heat transfer and the frequency of detachment. As long as the frequency is greater, the heat transfer increases. Most of the heat transfer is induced by the liquid movements associated with the vapor bubble detachment.

Key-words: - film boiling, volume of fluid, Computational Fluid Dynamics (CFD), bubble dynamics, Bubble behavior.

Received: May 24, 2022. Revised: January 11, 2023. Accepted: February 19, 2022. Published: March 20, 2023.

1 Introduction

Simulation film boiling is a computational technique used to model the process of film boiling, it generally occurs when a liquid comes into contact with a surface that is much hotter than the liquid's boiling point. In this process, a layer of vapor, which is formed between the hot surface and the liquid, reduces the contact area and slows down the heat transfer process. To simulate film boiling, researchers resort to creating a virtual model of the system by employing numerical methods and computer algorithms. The model takes into account various factors such as the fluid properties, the surface temperature, and the system`s geometry. Then, the model has been used to predict both how the fluid will behave under different conditions and to study the heat transfer process.

Simulation film boiling can be used to investigate various aspects of the phenomenon, such as the heat transfer rate, the formation of vapor bubbles, and the stability of the system. It can also be used to design and optimize heat transfer systems for various applications, such as nuclear reactors and electronic cooling systems.
simulation film boiling is a powerful tool that enables researchers to gain a deeper understanding of heat transfer in extreme conditions and to design more efficient and reliable heat transfer systems.
there are several methods for simulating film boiling, including computational fluid dynamics, finite element method, analytical models, and experimental methods. The choice of method will depend on the specific application and the available computational resources.

Computational Fluid Dynamics (CFD) simulations can be used to model the formation of vapor bubbles, the transfer of heat between the surface and the fluid, and the behavior of the fluid under different conditions. CFD simulation, which is recognized today as one of the essential design tools, is widely used. The choice of using this numerical method will essentially depend on the

type and complexity of the problem to be solved: the nature of the fluid, the thermodynamic behavior, and the modeling of the medium.
The equations governing the movements of a fluid, reflecting the conservation of both the energy (Navier-Stokes equations) as well as the fluid`s mass and momentum are solved by the numerical flow simulation codes or CFD codes. It can be observed that most of these codes use the finite volume method.

In this paper, avapor–liquid phase change model is proposed for the volume-of-fluid (VOF) method in FLUENT, [1], which code is the world's most widely used CFD software. The use of this code is not limited only by its functions, but it provides the user with the possibility for adding functions and defining all the peculiarities of his problem. It is a program based on C or C++ language that allows it to automate certain procedures such as boundary conditions, periodic, or others. This is achieved through the use of UDFs (User Defined Function) characteristic which will be compiled by an integrated compiler to be then executed, [2].

In Fluent, the VOF method solves a transport equation for one of the fluids volume fractions in each computational cell of the simulation domain. The fraction volume is defined as the fluid volume ratio in the cell to the total cell volume. The transport equation is solved iteratively over time, taking into consideration the advection and diffusion of the fluid interface, the effects of surface tension, gravity, and other relevant physical phenomena.

Film boiling is an important heat transfer phenomenon, which is characterized by the formation of a continuous vapor film on a heated wall. It is a two-phase flow heat transfer regime in which the bulk liquid is separated from the heating surface by a thin layer of continuous vapor film**.** Film boiling is a major heat transfer mechanism that occurs when the wall temperature is much higher than the saturation temperature of the liquid. Several methods have been developed to study film boiling phenomena, such as theoretical models, experiment correlations, and numerical simulations, [3], [4], [5], [6], [7].

To estimate the heat transfer process, diverse theoretical models for film boiling have been developed in the literature. The transfer flux can be predicted using an approach introduced by Berenson, [8], This approach takes into consideration the concept of hydrodynamic instabilities which was later developed by Zuber to describe the heat flux. This approach, which describes film boiling, associates the onset of vapor bubbles with the appearance of Taylor- type interfacial instabilities. This model was notably developed by Berenson as a continuation of Zuber's work, considering the case of a flat plate.

2 Numerical Method

The vapor phase is usually generated in the thin film region on the lower portion of the surface and is removed upward through the formation and release of bubbles. The vapor layer of density ρ_l and thickness δ is topped by a liquid of density. The interface between them, with surface tension σ, is initially flat. The evolution of the vapor-liquid interface during film boiling on a horizontal surface is determined by Taylor instability, [9].

When the vapor film thickness is weak and the liquid and vapor velocities can be neglected. In this case, stable disturbances are those whose wavelength is less than the value, [10], [11], [12], [13], which is defined as

$$\lambda_c = 2\pi\left(\frac{\sigma}{(\rho_l-\rho_v)g_y}\right)^{1/2} \quad (1)$$

When all wavelengths can appear on the interface, the most likely value is the one with the most rapid growth. This wavelength is referred to as the dominant or the most dangerous one, [14], [15].

$$\lambda_0 = 2\pi\left(\frac{3\sigma}{(\rho_l-\rho_v)g_y}\right)^{1/2} \quad (2)$$

The progression of the interface between the phases is accomplished by the solution of the following equation (for the q^{th} phase), [16], [17], [18], [19], [20], [21].

$$\frac{\partial \alpha_q}{\partial t} + \vec{v}\nabla\alpha_q = \frac{S_{\alpha_q}}{\rho_q} \quad (3)$$

$$\frac{\partial}{\partial t}(\rho\vec{v}) + \nabla(\rho\vec{v}\vec{v}) = -\nabla p + \nabla\left[\mu\left(\nabla\vec{v} + \nabla\vec{v}^T\right)\right] + \rho\vec{g} + \vec{F} \quad (4)$$

$$\nu = \frac{\alpha_1\rho_1\nu_1 + \alpha_2\rho_2\nu_2}{\rho} \quad (5)$$

$$\frac{\partial}{\partial t}(\rho E) + \nabla\left(\vec{v}(\rho E + p)\right) = \nabla\left(\lambda_{eff}\nabla T\right) + S \quad (6)$$

S is a source of the latent heat due to phase change at the interface, [22].

$$E = \frac{\sum_{q=1}^{n} \alpha_q \rho_q E_q}{\sum_{q=1}^{n} \alpha_q \rho_q} \quad (7)$$

The term source S is the volumetric term of the heat The general form of the mass source in the vapor phase is

$$S_{\alpha_v} = \frac{(q_v'' - q_l'').\nabla \alpha_l}{h_{lv}} \quad (8)$$

The difference in heat flow is approximately given as the source.

$$(q_v'' - q_l'') \approx (\alpha_l \lambda_l - \alpha_v \lambda_v)\nabla T \quad (9)$$

With this approximation, equation (8) becomes

$$S_{\alpha_v} = -\frac{(\lambda_l \alpha_l + \lambda_v \alpha_v)(\nabla T \cdot \nabla \alpha_l)}{h_{lv}} \quad (10)$$

Since there is no internal mass source, the mass source of the liquid phase becomes

$$S_{\alpha_l} = -S_{\alpha_v} \quad (11)$$

The latent heat source for the energy equation becomes:

$$S_E = -S_{\alpha v}.h_{lv} \quad (12)$$

3 Computational Domain and Simulation Condition

In recent years, several studies have been made to clarify and model the boiling mechanism that is associated with the liquid-vapor phase change process in the nucleate boiling regime. An interesting regime which is film boiling is discussed when the increase in temperature implies an increase in heat flux.

In the phase change problem, the equations for continuity, energy, and mass generally need to include surface tension effects, latent heat, interface mass transfer, and liquid-vapor dynamics.

The computational domain in film boiling refers to the area of the simulation that is used to model the heat transfer and fluid dynamics of the process. Boundary conditions for the simulation, such as the temperature and pressure at the boundaries of the liquid and vapor regions have been added. These boundary conditions are essential for accurately modeling the heat transfer and fluid dynamics of the film boiling process.

The simulation conditions for film boiling include the properties of the liquid and the vapor, the boundary conditions, and the heat flux or temperature of the heated surface. The properties of the liquid and vapor are typically modeled using thermodynamic models, such as the ideal gas law or the Antoine equation. Also, parameters such as density, viscosity, thermal conductivity, and specific heat can be included. For the simulation domain, the width along the x-axis will be equal to the wavelength of the Rayleigh–Taylor instability (λ_0) to allow visualization of the rise of a single vapor bubble. Rayleigh–Taylor instability is one of the important theories, which has been usually analyzed for inviscid flows.

An inviscid flow analysis is acceptable for general circumstances. Taking advantage of the flow symmetry, the width of the computational domain is chosen to be $\lambda_0/2$, and the height of the domain is $3\lambda_0/2$, to visualize the behavior of the ascent and to have only one bubble at a time. The initial thickness of the film is maximum at "x = 0" defined as "node" and minimum at $x = \lambda_0/2$ defined as "antinode". The boundary conditions on the two left and right faces of the domain are symmetric boundary conditions, [23], [24], [25].

The initial shape of the vapor-liquid interface is disturbed by the formation and the increase of the bubble. So, there is another initialization of the UDF function in which the steam-filled cells must meet certain conditions, [26].

In film boiling, a thin layer of vapor film of thickness δ(x) is formed over a horizontal flat plate due to the rapid boiling of the liquid film that initially covers the plate. The thickness of the vapor film varies along the plate in the x-direction due to variations in the local heat flux and fluid properties. The thickness of the vapor film is an important parameter that affects the heat transfer rate and the stability of the boiling process. The vapor film acts as a thermal insulator, reducing the rate of heat transfer from the plate to the fluid. However, if the thickness of the vapor film is too large, it can become unstable and break down, leading to the formation of vapor bubbles and the transition to nucleate boiling, [27].

$$\delta = \frac{\lambda_0}{64}\left(4 + cos\frac{(2\pi x)}{\lambda_0}\right) \quad (13)$$

at $x = 0$: $u = 0, \quad \frac{\partial v}{\partial x} = 0, \quad \frac{\partial T}{\partial x} = 0, \quad \frac{\partial \alpha}{\partial x} = 0$

at $x = \frac{\lambda_0}{2}$: $u = 0, \quad \frac{\partial v}{\partial x} = 0, \frac{\partial T}{\partial x} = 0, \quad \frac{\partial \alpha}{\partial x} = 0$

Boundary conditions at the exit on the upper surface of the domain:

at $y = \frac{3\lambda_0}{2}$: $\frac{\partial u}{\partial y} = \frac{\partial v}{\partial y} = \frac{\partial T}{\partial y} = \frac{\partial \alpha}{\partial y} = 0; \quad P = P_0$

at $y = 0$: $\quad T = T_{sat} + \Delta T_{sat}$

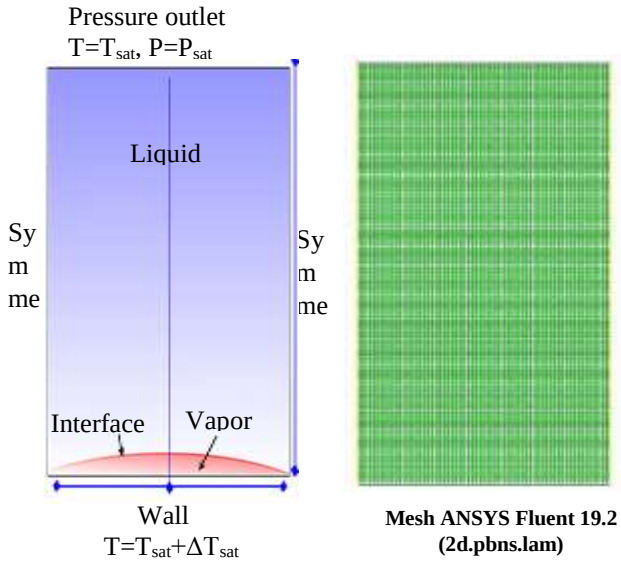

Fig. 1: Mesh and boundary condition

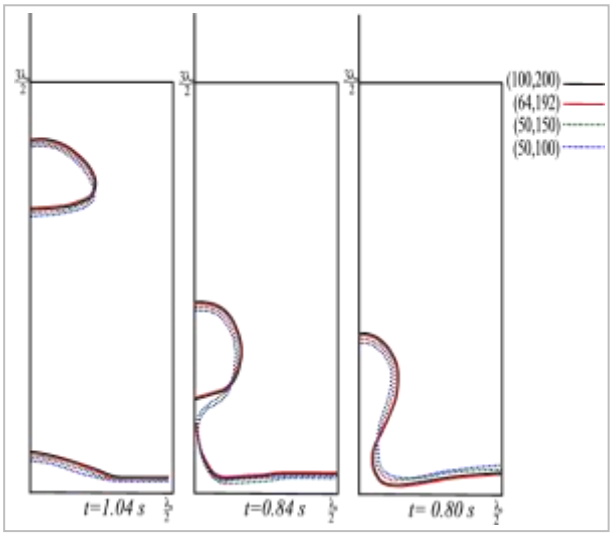

Fig. 2: Evolution of a bubble for different meshes.

Fig.1 presents the mesh and boundary condition. Moreover, regarding the choice of mesh, Fig.2 shows the different meshes tested (mesh (64,192) is the most suitable).

3.1 Evolution of a Steam Bubble during its Ascent

The evolution of a steam bubble during its ascent in film boiling simulation is highly dependent on the local flow conditions and heat transfer mechanisms, as well as the properties of the fluid and the heated surface. Accurately capturing these phenomena in simulation requires careful modeling of the relevant physical processes and a high-quality mesh that can resolve the steep gradients in temperature, pressure, and velocity.

A set of images about steam bubble life cycles from birth to disappearance is presented in Fig.3 below, and this is for different values of superheat ΔT_{sat} equal to 5°C, 10°C and 15°C. From these images it can be concluded that superheat plays a very important role in increasing the cyclic frequency of detachment of a steam bubble; therefore, superheat actively participates in the increase of heat flow. For a superheat of 5°C and time equal to 1.6s, there has been a single life cycle of a vapor bubble. For 10°C, two life cycles have been obtained, whereas, three cycles have been obtained for 15°C. During the life cycle of a steam bubble, it is found that the shape of the bubble is not always spherical; however, there is a change in the shape of the steam bubble from a hemispherical shape to a cap shape, [28]. It is also found that the detachment time is inversely proportional to the superheat of the wall. In addition, the bubble detachment from the hot surface affects the steam film, thus improving the heat transfer.

The increase in superheat increases the frequency of bubble formation but also ensures film boiling.

The evolution of the volume fraction, the field of temperatures, and velocities around the rising bubble
which were taken at various times and are presented in Fig.4, Fig.5, and Fig.6.

Time	ΔT_{sat}=5°C	ΔT_{sat}=10°C	ΔT_{sat}=15°C
t=0.1s	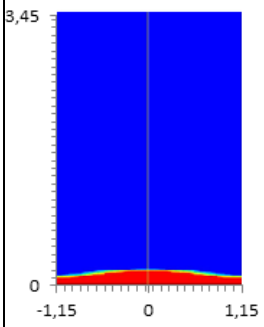	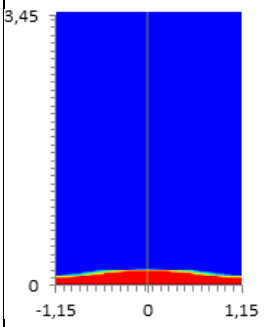	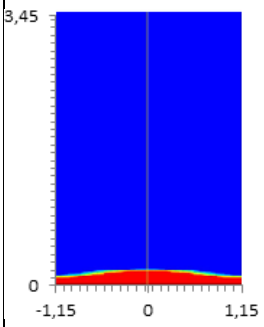
t=0.6s	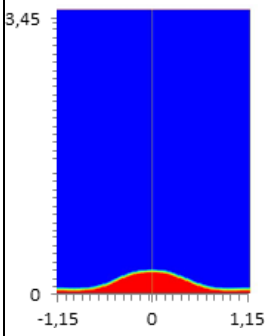	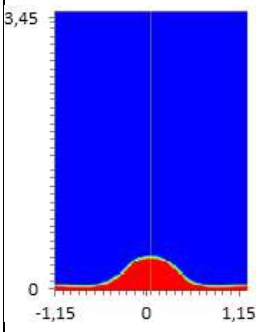	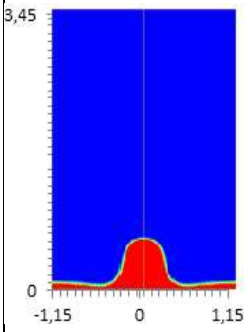
t=0.7s	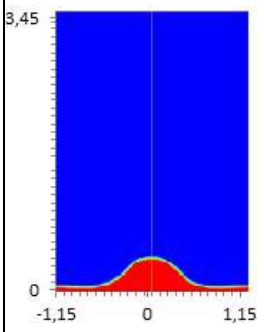	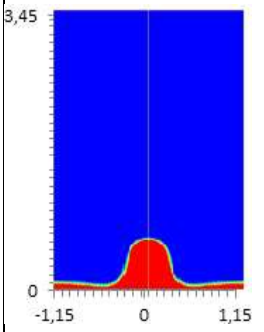	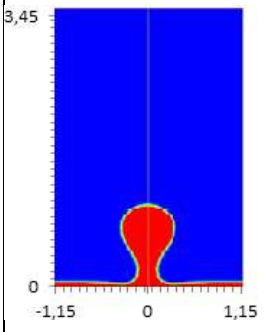
t=0.8s	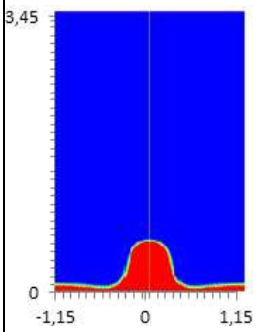	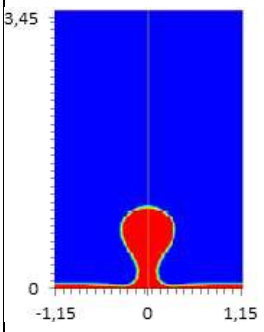	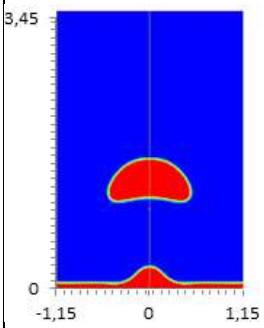

Fig. 3: Detachment profile of a vapor bubble at different steps time for different superheat values.

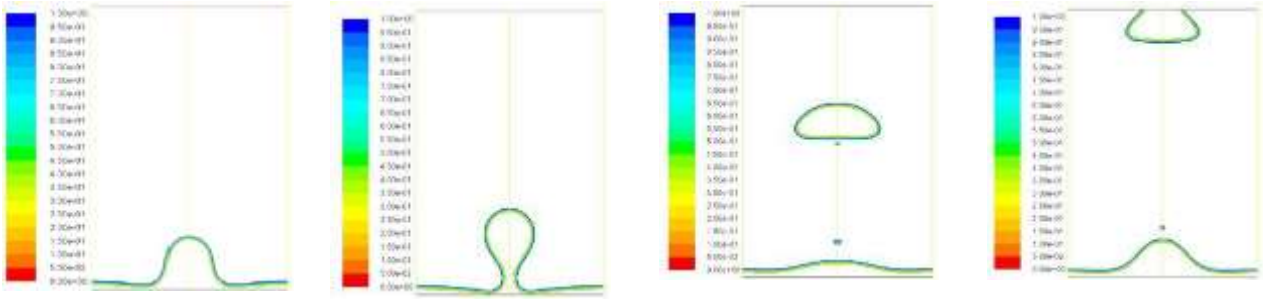

t=0.7s t=0.8s t=1 s t=1.2s

Fig. 4: Contour of the volume fraction

During the ascent of a steam bubble, the diameter at the base of the bubble begins to shrink and then the shape of the bubble flattens. After a time, equal to 1.2s, the detachment process ends and the next cycle begins. The experiments of [29], demonstrate that the second bubble is formed when the first is released. This behavior of the bubbles is precisely revealed by this simulation. Fig.4 shows the volume fraction contours of the vapor bubble for this specific case. This phenomenon can be described in the following detail: In the initial period, the bubble takes on a hemispherical shape. When it is growing, the liquid fills the space between the bubble and the interface by pushing the interface down, therefore, the bubble changes shape and becomes quasi-spherical. Then, the bubble detaches and moves away evacuating the energy stored in the form of latent heat of vaporization in the near wall. Therefore, a new cycle will begin. As the ascent progresses, it is observed that the bubble takes the form of a spherical cap, which is more spread out in width and less extended in length. The surface tension plays a very important role in highlighting the shape of the bubble.

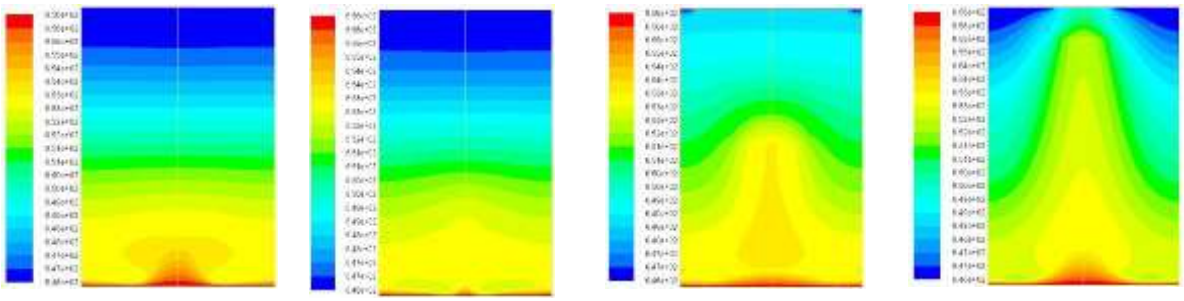

t=0.7s *t=0.8s* *t=1.0s* *t=1.2s*

Fig. 5: Temperature Distribution(K)

Fig.5 indicates that the temperature reaches a maximum value equal to 656.15°K at the level of the steam film and it also reaches high values around the bubble. However, in the upper part of the domain which is not affected by the movement of

the steam bubble, the temperature decreases until it reaches the T_{sat} (pressure outlet condition). For a time equal to t= 1s and t = 1.2s, a thermal wave that forms in the wake at the back (bottom) of the ascending bubble was observed. The distribution of temperatures of high values is in the form of a pyramid, the temperature remains minimal at the upper top of the antinodes.

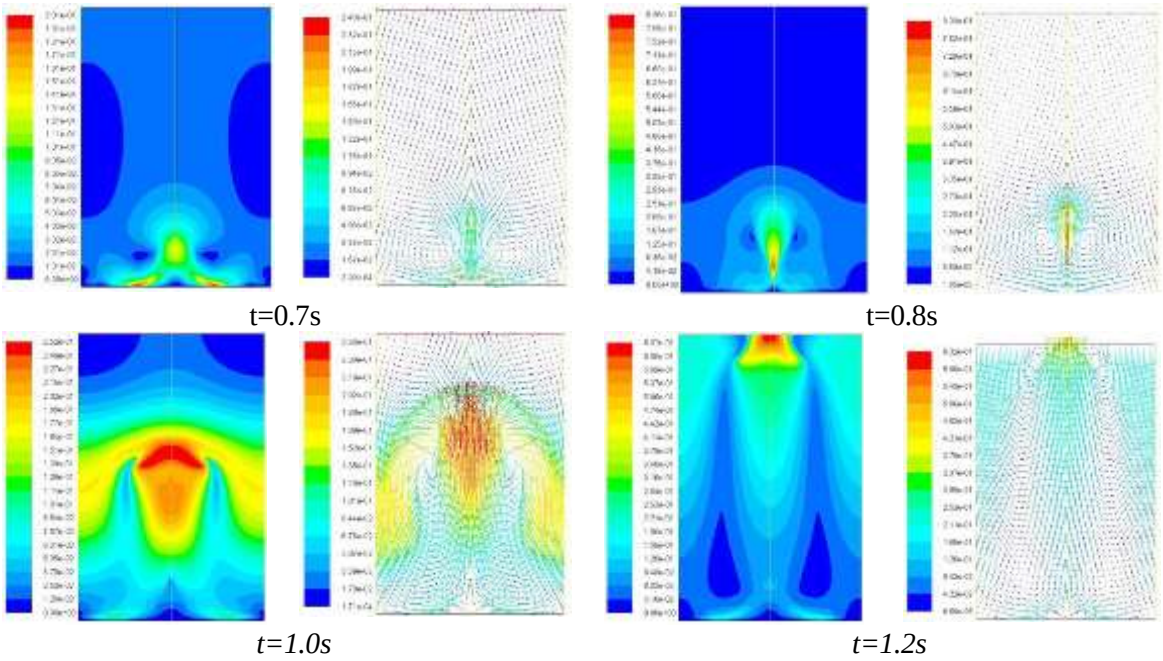

Fig. 6: Velocity Distribution (m/s)

Fig.6 shows the variation in the liquid velocities around the steam bubble during its birth, detachment, and ascent. For a time, equal to 0.7 seconds, it was noted that the velocity of the fluid is higher at the heart of the bubble in addition to the formation of symmetrical counter-rotations (vortexes) to mix the hot and cold steam located on both lateral sides of the wake of the bubble. Minimum velocities are located at the heart of these cells, at the lower antinodes, and at the point of birth of the bubble (node). During its growth, the hemispherical bubble attracts all the liquid around it thus increasing its speed (the hot vapor is transported to the lower parts of the bubbles, whereas, the cold vapor is transported to the bubble cap). For a time equal to 0.8 seconds, the cells against rotators are moved slightly upwards thus directing the maximum velocity vectors towards the axis of the anode, (the maximum velocities of the fluid are located just above and around the bubble by pulling it upwards). The direction of the velocities is practically parallel to the bubble direction movement, except in the lateral regions.

The velocity of the fluid is almost zero in the upper part since the influence of the increase in the steam bubble is negligible, However, it is maximum reaching 0.95m/s before the moment of the bubble detachment. For a time, equal to 1 second, the steam bubble is ascending and the maximum velocity of the fluid decreases reaching a value of 0.25 m/s, this is due to the expansion effect of the bubble and the maximum velocity vectors, which are located at the heart and around the bubble.

For the time of 1.2 seconds, when the bubble has touched the free surface and reached the value of 0.63m/s, the velocity of the fluid around the bubble increases. It can be seen that all the fluid is influenced by the movement of the ascending bubble as well as the one being formed. These results are similar and in line with the results obtained by [30].

3.2 Steam Bubble Velocity Movement

Fig.7 shows the maximum velocity at the heart of the bubble as a function of time. For each life cycle of a vapor bubble, two successive peaks represent the formation, detachment, ascent, and disappearance of the bubble. The velocity of the

bubbles which is almost identical for each cycle is maximum with values reaching 0.9m/s at the time of detachment. It is low when the bubble is rising with values between 0.25-0.35 m/s. The maximum velocity of the first bubble is lower than that of the subsequent bubbles.

These findings are also observed in the experiments of [28], who noticed that the second bubble is formed when the first is released. This second bubble is driven and lengthened by the circulatory movement created behind the first bubble which thus pulls it faster from the heating surface.

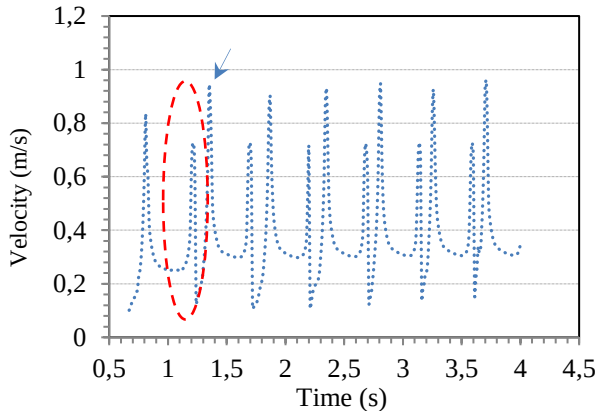

Fig. 7: Bubble velocity during their life cycles.

3.3 Nusselt Number Behavior

Nusselt represents the most important dimensionless number that characterizes the boiling phenomenon. It is defined as:

$$Nu = \frac{q.\lambda_0}{\lambda_l\left(T_p - T_{sat}\right)} \qquad (14)$$

The heat flux and the Nusselt number are proportional. This explains the behavior of the vapor bubble dynamics by linking the two parameters.
Fig.8 and Fig.9 represent the evolution of the Nusselt number as a function of time for different superheat values. The simulation carried out at different superheats of 5°C, 10°C, and 15°C, shows a significant variation in the number of peaks in the Nusselt number distribution.

A comparison between the mean Nusselt values (Nu_{avg}) of our simulation with those of the correlations of [14], [31], are represented in Fig.8, According to Fig.8, there is a similarity between the simulation results and those of the two correlations, with low errors between (6% - 12%).

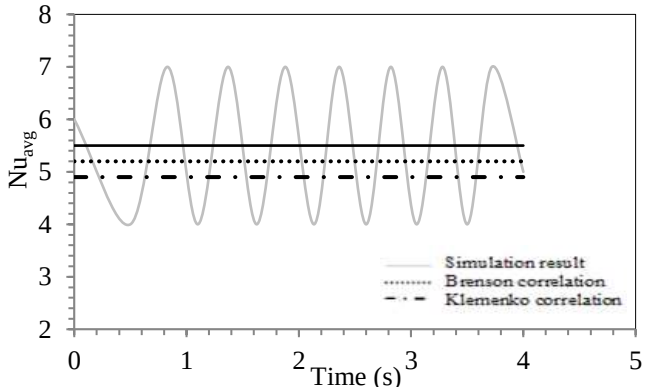

Fig. 8: Variation of the average Nusselt number ($\Delta T_{sat} = 10°C$).

These figures show the distribution of the number represented by individual peaks. These peaks indicate the life cycle of a vapor bubble, whereas, and the number of peaks indicates the number of bubbles formed during a determined time (in our case t=4 seconds).

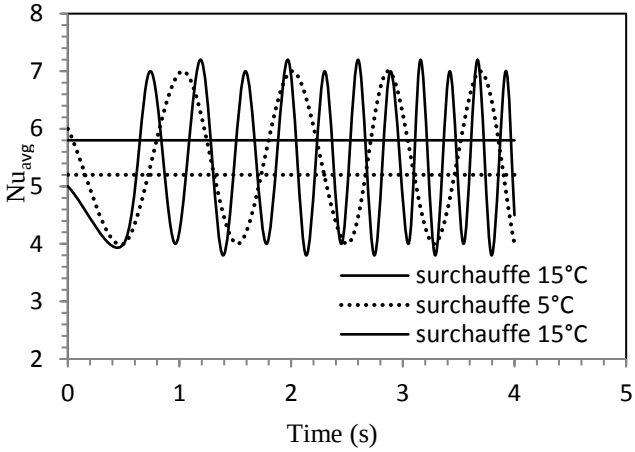

Fig. 9: Variation of the average Nusselt number

For superheat equal to 5°C, four peaks are observed indicating the formation of four vapor bubbles. For superheat, 10°c and 15°C seven bubbles and eleven bubbles were formed respectively. The study of the frequency of vapor bubble detachment, which is indicated by the temporal variation of Nu number, shows that for a superheat equal to 5°C, every second there is an average of one bubble with an initial detachment time equal to t_d=0.9s. For superheating at 10°C and with a lower detachment time t_d=0.83s, we have a detached bubble with an average of every 0.55s. Finally, for a superheat of 15°C the initial detachment time decreases again reaching the value t_d=0.7s, and the frequency of detachment of a bubble occurs with an average of every 0.35s. It is concluded that the increase in superheat implies an increase in the frequency of the

vapor bubble detachment. Hence, the Nu number and the heat flux are strongly dependent on the vapor film thickness. Nu and q are high when the vapor film thickness is thin and vice versa. Therefore, the average heat flux increases as more vapor rushes to fill the bubble, and the film becomes vapor deficient which leads to the reduction of its thickness resulting in a higher Nu number.

3.4 Effect of the High Superheat

the superheat at the heated surface can affect the shape and behavior of the vapor bubbles that form in the liquid. High superheat conditions can lead to the formation of large, unstable vapor bubbles that can be more difficult to control than smaller bubbles. the effects of high superheat on the shape and behavior of vapor bubbles in film boiling can be complex and dependent on many factors, including the geometry of the heated surface, the fluid properties, and the specific superheat conditions. Understanding these effects is important for designing and optimizing film boiling systems for various applications. The shape of the vapor bubbles can also be affected by the superheat conditions. In high superheat conditions, the bubbles can take on irregular shapes. This can affect the heat transfer characteristics of the system and can also affect the behavior of the vapor film.

Fig.10 shows the influence of high superheat on the steam film for the same conditions considered above, and this for different superheat values: 20°C, 30°C, and 100°C.

At high superheat, after the detachment of the first steam bubble a second bubble of small size is formed. It is first attached to the steam rod and then it detaches in turn. A third bubble also attached to the steam is

then formed which is always of small size After a fraction of a second, we have coalescence of the second and the first bubble. After the disappearance of the first bubbles, the third in turn detaches from the steam. Then, another bubble of the same dimension is formed as the third detaches with a more or less rapid time. This phenomenon continues, with a detachment of the bubble being done at a lower position for steam of lower height. The diameters of the latter bubbles are small and then pass to medium dimensions.

It is found that at high superheat, a large amount of steam is generated in which the steam bubble takes the shape of a fungus. These results have also been observed experimentally by [32].

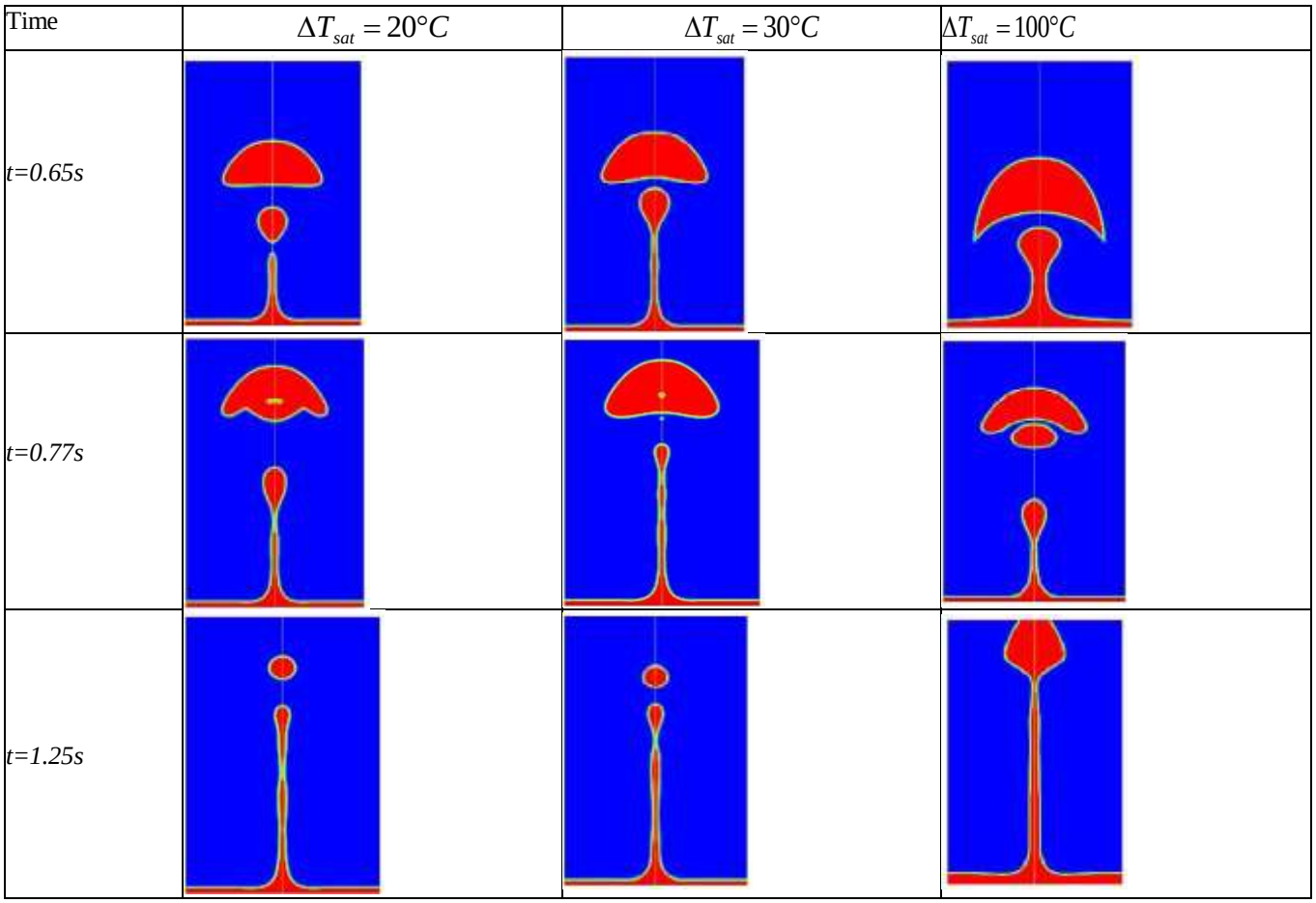

Fig. 10: Evolution of steam film with high superheat

Fig.11 below shows the relationship between the detachment time of the first steam bubble and superheat, we note that the detachment time of the first vapor bubble decreases with the increase in the wall
superheat and this at low superheat. But at high superheat (i.e. superheat above 20°C), the detachment time is almost identical with values between (0.47-0.55) seconds.

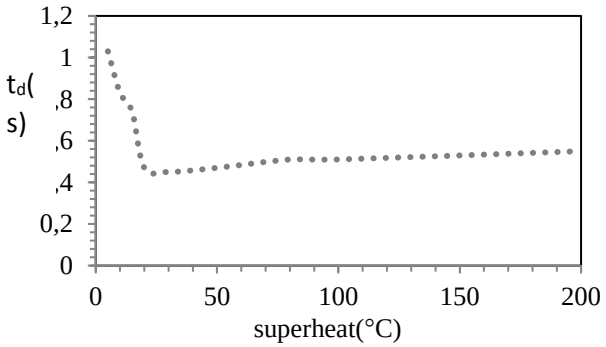

Fig. 11: Initial detachment time as a function of superheat

4 Conclusion

This study includes a numerical simulation of the boiling phenomenon, which allows a better understanding and a complete visualization of the growth dynamics of vapor bubbles. By simulating this process, researchers can gain a better understanding of heat transfer in extreme conditions and how to improve heat transfer efficiency in various applications. This simulation using the fluid volume method (VOF), presents the evolution of vapor bubbles (birth, detachment, ascent, and disappearance) by velocity, temperature, and volume fraction profiles. The evolution of the Nusselt number, depending on the different control parameters, such as time and superheat, is also shown. Several suggested improvements were included in this study, counting incorporating effects of different parameters (surface dimension, superheat, Nusselt number), adaptive mesh refinement, and high-performance computing. Incorporating these improvements enhance the accuracy and efficiency of film boiling simulations, and enable more accurate predictions of film boiling behavior in real-world systems. This study was evaluated and validated by comparison with

numerical correlations where it showed good agreement. The simulation results reveal that the increase in superheat implies an increase in the frequency of vapor bubble detachment. The value of the Nusselt number is maximum at the point of bubble detachment. The superheating plays a very important role in increasing the cyclical frequency of bubble detachment and thereby increasing heat flux. The study of the bubble dynamics has also concluded that the detachment of the bubble from the heating surface disturbs the vapor film and therefore improves the heat transfer. When the boiling phenomenon is studied at the scale of an individual bubble, it is often considered to be spherical. This assumption facilitates the exhaustive numerical computation necessary in solving the Naviers-Stokes equations. However, from our study, it was observed that the shape of a boiling bubble is not spherical due to the different forces acting on it. Then, we can distinguish a change in the shape of the vapor bubble, going from a spherical and hemispherical shape to a shape of a cap and a mushroom. The study of the vapor bubble detachment frequency indicated by the temporal variation of the Nu number and presented by peaks shows that there is an inversely proportional relationship between both the Nu number and the heat flux with the vapor film thickness; therefore, heat transfer is important for a thin vapor film. At high superheat and as a large amount of vapor is generated, the vapor bubbles break off with different sizes thus forming a vapor rod along the domain. It is also noted that the high values of the superheat lead to the rapid formation of the vapor, this consequently causes the attachment of these bubbles with the vapor rod. The dimensions of the computational domain are determined from the wavelength of the Rayleigh-Taylor instability. The variation of these dimensions influences the volume of the bubble, the time of detachment, the distribution of temperature, the velocity, and the rate of heat transfer. We can therefore conclude that the wavelength of the Rayleigh-Taylor instability is the governing length scale; this is on the dimensions, the number, and the detachment time of the bubbles. Consequently, the characteristics associated with the bubble, such as its volume, its cyclic frequency, and its thermal transport, are interrelated.

Future directions

In terms of future directions in studying numerical simulation in film boiling, there are several ongoing research efforts focused on advancing this field by developing more accurate models in terms of modeling the various physical processes that occur during film boiling. For example, models could be developed that account for the effects of surface roughness, bubble coalescence, and other factors that can affect the heat transfer and fluid dynamics., expanding the range of geometries that can be studied, investigating multiphase flow, and validating simulation results against experimental data.

Abbreviations:

c	$Jkg^{-1}k^{-1}$	*Specific heat*
D	m	*wall length*
d	m	*Bubble diameter*
f	s^{-1}	*Frequency*
g	ms^{-2}	*Gravitationnel acceleration*
h	$wm^{-2}k^{-1}$	*Heat transfer coefficient*
h_{lv}	Jkg^{-1}	*Latent heat of vaporization*
L_c	m	*Capillary length*
p	*Pa, atm*	*Pression*
S	-	*Source term specific to phase change*
T	k	*Temperature*
t	s	*Time*
t_d	s	*Detachment time*
v	m/s	*Velocity*
ΔT	k	*Superheat*
δ	m	*Vapor film thickness*
λ	m	*Wavelength*
μ	$Kg\ m^{-1}s^{-1}$	*Dynamic viscosity*
υ	m^2s^{-1}	*Kinematic viscosity*
ρ	Kgm^{-3}	*Density*
σ	Nm^{-1}	*Surface tension*

References:

[1] Fluent 6.0 Users Guide Documentation, Fluent Inc, 2001.

[2] Moritz Eickhoff, Antje Rrücker, Solidification modeling with user defined function in ansys fluent, *International Conference on Computational Fluid Dynamics in the Oil & Gas*,2017.

[3] Yue Jin , Koroush Shirvan, Study of the film boiling heat transfer and two-phase flow interface behavior using image processing, *International Journal of Heat and Mass Transfer,Vol.177*,2021, pp.121517.

[4] Thanh-Hoang Phan, Cong-Tu Ha, Numerical simulation of bubble collapse between two parallel walls and saturated film boiling on a sphere, *International Journal of Heat and Mass Transfer*, Vol. 127,2018, pp.116–125.

[5] Yue Jin, Koroush Shirvan, Study of the film boiling heat transfer and two-phase flow

interface behavior using image processing, *International Journal of Heat and Mass Transfer*,Vol.177, 2021,pp.121517.

[6] Xiuliang Liu, Qifan Zou, Ronggui Yang, Theoretical analysis of bubble nucleation in liquid film boiling, *International Journal of Heat and Mass Transfer*, Vol.192, 2022, pp.122911.

[7] Fella Chouarfa, M.Hocine Benhamza, and Malek Bendjaballah, New model of heat transfer in the process of nucleate boiling in a pool: prediction and assessment,*journal of engeneering physics and thermophysics*, Vol.87, 2014, pp.721-729.

[8] P. J. Berenson, Film Boiling Heat Transfer from a Horizontal Surface, *Journal of Heat Transfer*, Vol. 83, 1961, pp.351-356.

[9] G. Son V. K. Dhir, Numerical Simulation of Saturated Film Boiling on a Horizontal Surface, *Journal of Heat Transfer*,Vol.119, 1997, pp. 525-533.

[10] Dong-Liang Sun, Jin-Liang Xu, Li Wang, Development of a vapor–liquid phase change model for volume-of-fluid method in FLUENT, *International Communications in Heat and Mass Transfer*, Vol.39 2012, pp.1101-1106.

[11] Yohei Sato, Bojan Niceno, Pool boiling simulation using an interface tracking method: From nucleate boiling to film boiling regime through critical heat flux, *International Journal of Heat and Mass Transfer*,Vol.125, 2018, pp.876-890.

[12] Boltezman: Xiaojing Ma, Ping Cheng, Xiaojun Quan, Simulations of saturated boiling heat transfer on bio-inspired two-phase heat sinks by a phase-change lattice Boltzmann method, *International Journal of Heat and Mass Transfer*,Vol.127, 2018, pp.1013–1024.

[13] Seyed Amirreza Hosseini, Ramin Kouhikamali, A numerical investigation of various phase change models on simulation of saturated film boiling heat transfer, *Heat Transfer Asian Research*,Vol.148, 2019, pp.2577-2595.

[14] V.P. Carey, Liquid-Vapor Phase-Change Phenomena: An Introduction to the Thermophysics of Vaporization and Condensation Processes in Heat Transfer Equipment, Taylor & Francis Group, New York, 2008.pp.730.

[15] Lining Donga,b , Shuai Gonga , Ping Cheng ,Direct numerical simulations of film boiling heat transfer by a phase-change lattice Boltzmann method, *International Communications in Heat and Mass Transfer*, Vol.91, 2018, pp.4923-4927.

[16] Djati Walujastono and Kouichi Kamiuto, Film Boiling Heat Transfer from a Horizontal Circular Plate Facing Downward, *Heat Transfer—Asian Research*, Vol.32 , 2003, pp.72.

[17] Yuan Feng, Numerical study on saturated pool boiling heat transfer in presence of a uniform electric field using lattice Boltzmann method, *International Journal of Heat and Mass Transfer*,Vol.135, 2019, pp.885–896.

[18] Q. Li, Y. Yu, P. Zhou, H.J. Yan, Enhancement of boiling heat transfer using hydrophilic-hydrophobic mixed surfaces: A lattice Boltzmann study, *Applied Thermal Engineering*, Vol. 132, 2018, Pages 490-499.

[19] Jun-young Kang and al, Minimum heat flux and minimum film-boiling temperature on a completely wettable surface: Effect of the Bond number, *International Journal of Heat and Mass Transfer*, Vol.120, 2018, pp.399–410.

[20] Anjie Hu, Dong Liu, 2D Simulation of boiling heat transfer on the wall with an improved hybrid lattice Boltzmann model, *Applied Thermal Engineering*, Vol.159, 2019, pp. 113788.

[21] Shaojun Dou, Liang Hao, Hong Liu, Numerical study of bubble behaviors and heat transfer in pool boiling of water/NaCl solutions using the lattice Boltzmann method, *International Journal of Thermal Sciences*, Vol.170, 2021, pp.107158.

[22] M.H. Yuan, Y.H. Yang, T.S. Li, Z.H. Hu, Numerical simulation of film boiling on a sphere with a volume of fluid interface tracking method, *International Journal of Heat and Mass Transfer*,Vol.51, 2008, pp.1646-1657.

[23] Byoung Jae Kim, Jong Hyuk Lee, Kyung Doo Kim, Rayleigh–Taylor instability for thin viscous gas films: Application to critical heat flux and minimum film boiling, *International Journal of Heat and Mass Transfer*,Vol.80, 2015, pp.150-158.

[24] Samuel W. J. Welch and Gautam Biswas, Direct simulation of film boiling including electrohydrodynamic forces, *physics of fluids*, Vol.19, 2007, pp.012106,.

[25] Shi-Wen Lin, Yin-Nan Lai, Feng-Chi Wu,Yeng-Yung Tsui, Phase change calculations for film boiling flows, International Journal of Heat and Mass

Transfer,Vol.70, 2014,pp.745-757.
[26] A. Esmaeeli, G. Tryggvason, «Computations of film boiling. Part I: numerical method», *International Journal of Heat and Mass Transfer*, Vol.47, 2004, pp. 5451–5461.
[27] B. M. Ningegowda and B. Premachandran, Numerical Simulation of Two-Dimensional Forced Convective Film Boiling Flow over a Horizontal Flat, *Surface Procedia IUTAM* Vol.15, 2015, pp. 256-263.
[28] Kaikai Guo, Huixiong Li , Yuan Feng, Tai Wang, Jianfu Zhao, Numerical simulation of magnetic nanofluid (MNF) film boiling using the VOSET method in presence of a uniform magnetic field, *International Journal of Heat and Mass Transfer*, Vol.134, 2019, pp. 17-29.
[29] Shoji, M., Witte, L. C. and Sankaran, S « the influence of surface conditions and subcooling on film-transition boiling». *Exptl. Thermal Fluid Sci*, Vol.3,1990, pp.280-290.
[30] G. Tomar and G. Biswas, « Numerical simulation of bubble growth in film boiling using a coupled level-set and volume-of-fluid method», *Physics of fluids*, Vol.17, 2005, pp. 112103.
[31] V. Klimenko, Film boiling on a horizontal plate—new correlation, Int. *International Journal of Heat and Mass Transfer*. Vol.24 ,1981, pp.69–79.
[32] Ervin, J.S., Merte, H. Jr., Keller, R. B. and Kirk, K. «Transient pool boiling in micro-gravity. » *International Journal of Heat and Mass Transfer*, Vol.35, 1992, pp.659-674.

Contribution of Individual Authors to the Creation of a Scientific Article (Ghostwriting Policy)

The authors equally contributed in the present research, at all stages from the formulation of the problem to the final findings and solution.

Sources of Funding for Research Presented in a Scientific Article or Scientific Article Itself

No funding was received for conducting this study.

Conflict of Interest

The authors have no conflicts of interest to declare that are relevant to the content of this article.